

Human movement detection and classification capabilities using passive Wi-Fi based radar

Hidayatuserlina Razali¹, Nur Emileen Abd Rashid², Muhammad Nazrin Farhan Nasarudin¹,
Nor Najwa Ismail³, Zuhani Ismail Khan², Siti Amalina Enche Ab Rahim²,
Megat Syahirul Amin Megat Ali², Nor Ayu Zalina Zakaria²

¹School of Electrical Engineering, College of Engineering, Universiti Teknologi MARA, Shah Alam, Malaysia

²Microwave Research Institute, Universiti Teknologi MARA, Shah Alam, Malaysia

³NR Electrical and Electronic Enterprise, Semenyih, Malaysia

Article Info

Article history:

Received Sep 19, 2023

Revised Mar 12, 2024

Accepted Mar 15, 2024

Keywords:

Classification

Detection

Human movement

Leave-one-out cross-validation

Wi-Fi

ABSTRACT

Human detection and classification via Wi-Fi transmission have received a lot of attention in recent years as crucial facilitators in security and human-computer interaction (HCI). The passive Wi-Fi radar (PWR) system used by previous researchers applied cross-ambiguity function (CAF) and CLEAN algorithms to process the detected signals. This paper explores the feasibility and viability of a PWR system in detecting and classifying human movements without utilizing CAF and CLEAN algorithms. The movements are performed by four participants but with comparable body sizes and heights. Three daily human movements are investigated namely walking, bending, and sitting, with each participant performing each movement 24 times, providing a total of 96 samples per activity. The system is evaluated based on the consistency of the signal pattern in a frequency domain and the percentage accuracy is assessed using an artificial neural network (ANN) classifier and trained using a leave-one-out cross-validation (LOOCV) method. The frequency domain results reveal that the signals are consistent, with no noticeable variations or changes in the voltage intensity or shape of the main lobe. The classification of the movements shows that the classifier has an overall accuracy of 97.6%.

This is an open access article under the [CC BY-SA](https://creativecommons.org/licenses/by-sa/4.0/) license.



Corresponding Author:

Nur Emileen Abd Rashid

Microwave Research Institute, Universiti Teknologi MARA

40450 Shah Alam, Selangor, Malaysia

Email: emileen98@uitm.edu.my

1. INTRODUCTION

Passive radar systems for detecting targets employing opportunity illuminators have received a lot of interest recently. Early studies have utilized analogue transmissions such as very high frequency (VHF) radio [1] and ultra-high frequency (UHF) television broadcasts [2], [3] as opportunity illuminators. As digital processing has evolved, digital transmission has also increased in interest as the opportunity illuminators, such as a global system for mobile communications (GSM) [4], [5] and digital audio broadcasts/digital video broadcasts terrestrial (DAB/DVB-T) [6].

Nowadays, metropolitan areas have a large-scale deployment of Wi-Fi networks, and many public and private places are fitted with one or more Wi-Fi access points (AP). These Wi-Fi APs offer a variety of illumination sources, including the usage of a radar system. In recent years, passive Wi-Fi radar (PWR) has drawn increasing attention. It is fast expanding in coverage across a wide range of application industries, including military, security, healthcare, and transportation [7]–[9]. This is because Wi-Fi signals are

modulated using orthogonal frequency division multiplexing (OFDM), which has an ambiguity function that suggests appropriate accuracy [10]. Furthermore, the maximum usable bandwidth of the Wi-Fi signals is 160 MHz, which enables a resolution of about 1 m [11].

The earliest research on a PWR system was published in [12], where the system was employed for locating and tracking users inside a building utilizing 3 receivers, and it was discovered that the system is capable of locating and tracking users with a high level of precision. Other researchers have also implemented the PWR system in localizing and tracking moving targets by exploiting multiple passive sensors as reported in study [1]. Besides that, the PWR system has also been utilized in sensing human presence [13], [14]. Expanding the capability of the PWR system, researchers have also proved that fall events can be detected in real-time using a widely deployed Wi-Fi device at home [15]–[17]. In addition, the PWR system has also been used for context-awareness applications such as human activity detection and recognition.

In study [18], a power system is employed to simultaneously detect respiration and physical movements utilizing a wireless energy transmitter and two receivers. A primary receiver picks up signals directly from the source, whereas a secondary receiver picks up signals reflected off people in motion. This study aids in monitoring the activity of adults, which can be associated with their physical activity. The support vector machine (SVM) classifier was tested with three feature vectors and achieved an accuracy of 85%. Meanwhile, 3 basic activities were conducted in [14] where a commercial Wi-Fi router was positioned in a corner of the room as noncooperative illuminator and a receiver device was positioned outside the room, separated by a plywood partition board. The receiver device was equipped with two wideband horn antennas: one directed towards the Wi-Fi access point and the other directed towards the room area to detect human motion. In all instances, the Doppler effect of movements is readily identified with distinct characteristics that can be effortlessly applied for subsequent motion classification. In study [19], 3 volunteers were involved in human activity classification where the activities that the volunteers needed to perform were standing and walking. In the study, 2 types of information were used, namely Doppler and received signal strength (RSS). The Wi-Fi access point (AP) was positioned in one corner of the room, and the sensor was placed on an 80 cm high desk. One antenna was aimed towards the surveillance area as the surveillance channel, which gathered signals from both human and fixed objects; and the other at the Wi-Fi AP as the reference channel, which was used to reconstruct the sent Wi-Fi signal. At the end of the analysis, it was discovered that the Doppler information provided 95.3% accuracy while the RSS information created 69.3% accuracy using SVM classifier.

However, according to previous articles, the PWR system consists of reference and surveillance antennas that evaluate differences between reflected signals from the target and direct signals from the illuminator of opportunity. The second antenna complicates and bulks up the system, rendering it unsuitable for use as a monitoring system since the bulky system takes more space and is more difficult to move or carry as well as costly maintenance. Additionally, the cross-ambiguity function (CAF) and the CLEAN algorithms were used to process the collected signals. This results in a lengthy signal processing time. In contrast, the PWR system utilized in this investigation consists solely of surveillance antennas and does not employ the CAF or CLEAN algorithms. This strategy reduces the system's size and portability while enhancing its processing speed. The system also utilized a configuration based on forward scatter radar (FSR). Walking, bending, and sitting are performed by 4 volunteers with comparable body sizes and heights. Hence, the objective of this paper is to assess the practicability and viability of the PWR system for classifying the same human daily activities performed by different individuals without the reference antenna and additional algorithms.

2. HARDWARE CONFIGURATION AND EXPERIMENTAL SETUP

2.1. Hardware setup

The transmitter source in this work is a D-Link DSL-2640T wireless router which has an operational frequency range of 2.4 to 2.46 GHz. With a transmitter power of 16 dBm and a max gain of 2 dBi, the router can operate up to 100 m for indoor applications. An Alfa APA-M25 2.4+5 GHz dual-band indoor antenna with 8 dBi gain is included with the router. It is a directional patch antenna with a horizontal beam of 66° and a vertical beam of 16°. This type of antenna is utilized to avoid interferences from other directions. Meanwhile, the receiver consists of an antenna, a low noise amplifier (LNA), a diode detector, a low pass filter (LPF), and a data acquisition system (DAQ). The receiver's antenna is likewise a directional antenna, the Alfa APA-M25 2.4+5 GHz dual-band indoor antenna with 8 dBi gain. Figure 1 illustrates the receiver block diagram with its specification.

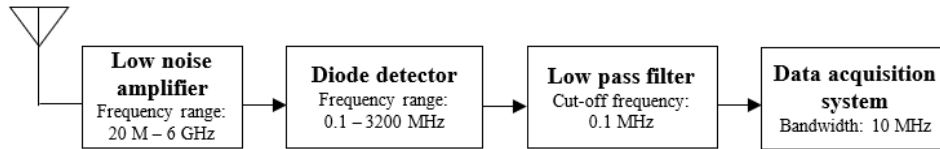


Figure 1. Receiver block diagram

2.2. Experimental layout

All experiments are carried out in an indoor laboratory room at the School of Electrical Engineering, College of Engineering, UiTM Shah Alam. The geometrical arrangement used is depicted in Figure 2 with top and side views. The transmitter and receiver are perpendicularly positioned at a 4.5 m distance baseline, resembling the FSR configuration, and 1.2 m above the ground. The red dot, point O , represents the starting center point where the participant stands before experimenting. The crossing point of the baseline is represented by O' and the final location for the participant to be after crossing 90° to the baseline, is at point O'' , which is 4.5 m from point O . As for a preliminary target signature detection, the crossing baseline is at 90° because it produces a symmetrical and ideal target signature compared to alternative trajectories [20].

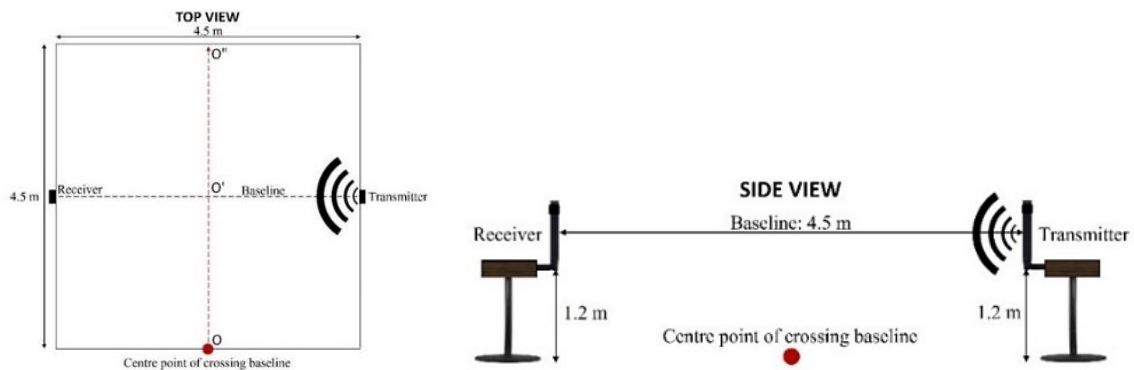


Figure 2. Experimental layout with top and side views

3. RESULTS AND DISCUSSION

In this section, it explains the results of the research and comprehensive discussion. Results can be presented in figures, graphs, tables and others that make the reader understand easily [21], [22]. The discussion can be made in several sub-sections.

3.1. Human activities

This experiment investigates three daily human movements, namely walking, bending, and sitting. There are no mobility restrictions as there are multiple ways to complete the task, including a few or many swinging hands, small or large walking steps, and the volunteers' pace/speed. The objective of this study is to observe the signal pattern of the respective activity as it is formed in different ways. To complete the activity, each participant will begin all activities at point O and end at point O'' .

3.2. Participants and number of data

In order to evaluate the sensor performance in capturing the signature of each activity, 4 volunteers, two males and two females ranging in age from 25 to 30 years old with very comparable body size and height participated in the data collecting. This is done to ensure the consistency of the signature even if it is executed by multiple participants but with the same criteria. Each individual collects 24 of 10-second samples with a frequency sampling, f_s of 10 kHz for each movement, for a total of 96 samples per activity.

3.3. Signal processing

Prior to signal processing, the collected signals are filtered with a Savitzky-Golay filter with the first polynomial order and 0.1 s window to eliminate extraneous noise. The collected pulsed (discrete) Wi-Fi signal is subjected to a cubic spline interpolation (CSI) procedure to fit all the data points and create a continuous and smooth curve that traverses x points. This will ensure that the intended signature can be seen

clearly. In comparison to other interpolations, CSI is superior at interpolating Wi-Fi signals [23]. The simplified formula for the CSI can be expressed by (1):

$$f(x) = a(x - x_1)^3 + b(x - x_1)^2 + c(x - x_1) + d \quad (1)$$

where [a, b, c, d] are the local coefficients and [x, x1] are the knot intervals.

The continuous (Doppler) signal, which is a time-domain signal, is then converted into a frequency-domain signal to further examine the properties of the signals by using a fast Fourier transform (FFT) technique. This technique is applied as the frequency components from the time-domain signals convey crucial details about the signal. The information or features of the signal will be gathered and displayed in the frequency-domain signal's primary lobes, while the signal's noise will be retained in the side lobes. The FFT is defined by (2) [24]:

$$X(k) = \sum_{n=0}^{N-1} x(n)e^{-j\frac{2\pi nk}{N}} \quad (2)$$

where $x(n)$ is the signal with transform length, $n=0 \dots N-1$, k is the N^{th} root of unity equal to $0 \dots N-1$, and N is the size of its domain.

From the frequency-domain signal, the features of the signal are extracted manually by dividing the primary lobes into 4 divisions with 2 Hz division by using a centroid-based method. The features are extracted from 2 components, which are voltage intensity and frequency. In this work, an artificial neural network (ANN) approach is applied to classify the signal characteristics. ANN operates by transmitting the value of the current neuron, y_{nth} in the current layer to all neurons on the following layer, y_{nth+1} via weight, w multiplication, and bias, b addition, which can be expressed by (3) [25]:

$$y_{n+1} = f x_n (b_n + \sum(y_n)(w_n)) \quad (3)$$

From the 4 divisions with 2 extracted components, therefore the input layer of the classifier is fed with eight (8). The hidden layer has 12 neurons, which appear to offer the best accuracy, while the output layer has three (3) neurons, which corresponds to the number of human movement classes. The number of epochs is 30.

To validate the accuracy of the classification of the signals, a standard mean absolute error (MAE) by leave-one-out cross-validation (LOOCV) is applied. It computes the average absolute difference between true ratings, y_i and prediction ratings, \hat{y}_i by utilizing one observation from the original sample as validation data and the rest observations as training data. This process is continued until each observation in the sample has been utilized as validation data once. The lower error values indicate better suggestion accuracy. The LOOCV is expressed by (4) [26]:

$$LOOCV = \frac{1}{n} \sum_{i=1}^n |y_i - \hat{y}_i| \quad (4)$$

3.4. Data analysis and discussion

Before commencing data collection, it is necessary to assess the availability and strength of the Wi-Fi signal. Figure 3 exhibits the spectrum measurement recorded at the receiver location. The absence of a Wi-Fi signal results in the absence of any observable peak, as seen by the red dotted line. Alternatively, a peak at 2.47 GHz with a signal-to-noise ratio (SNR) of ~39 dB, as seen by the blue line, occurs when the Wi-Fi router is switched ON. As the measurement will not be inferred by other signals, this suggests that the experimental region is appropriate for carrying out the measurements. Furthermore, even though the SA is at 4.5 m from the transmitter, the recorded SNR is still greater than 30 dB, which is reported to be excellent for Wi-Fi packet transfer [27].

The measured Wi-Fi signal without the presence of a target is shown in Figure 4(a). The inset clearly shows that the Wi-Fi transmissions are of the pulsed type, correlating with what has been reported in [10]. In the presence of a target, the measured signal is displayed in Figure 4(b). The graphic demonstrates the variation in signals that resulted from target movement. When the target blocks Wi-Fi transmission toward the receiver, the signal intensity, expressed in voltage (V), decreases. In Figure 4(c), the interpolated signal, which represents the Doppler signal of the crossing target, is plotted in the red line where the target signature is clearly visible.

Figures 5(a), 5(b), and 5(c) illustrate the time domain Doppler signals for walking, bending, and sitting, respectively. Every target movement generates a distinctive signature. The signature of each activity is separated into specific divisions to indicate the action as explained in detail in Table 1. The sitting activity forms more pronounced signatures compared to the other activities as demonstrated in Figure 5(c). This is

because seated activities are more complicated and require more actions to be performed than walking and bending activities.

Figure 6 compares the Doppler signals generated during walking, bending, and sitting. The comparison illustrates the distinct differences between the Doppler patterns of each activity. This demonstrates and verifies that the PWR system utilized in this experiment is functional and capable of capturing a variety of human motions by producing a distinct Doppler signal pattern.

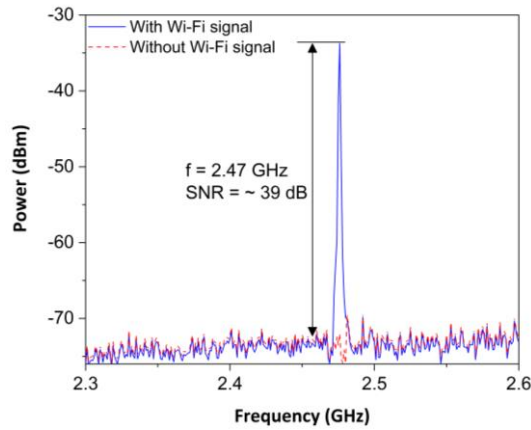


Figure 3. Display of the SA with and without the presence of a Wi-Fi signal

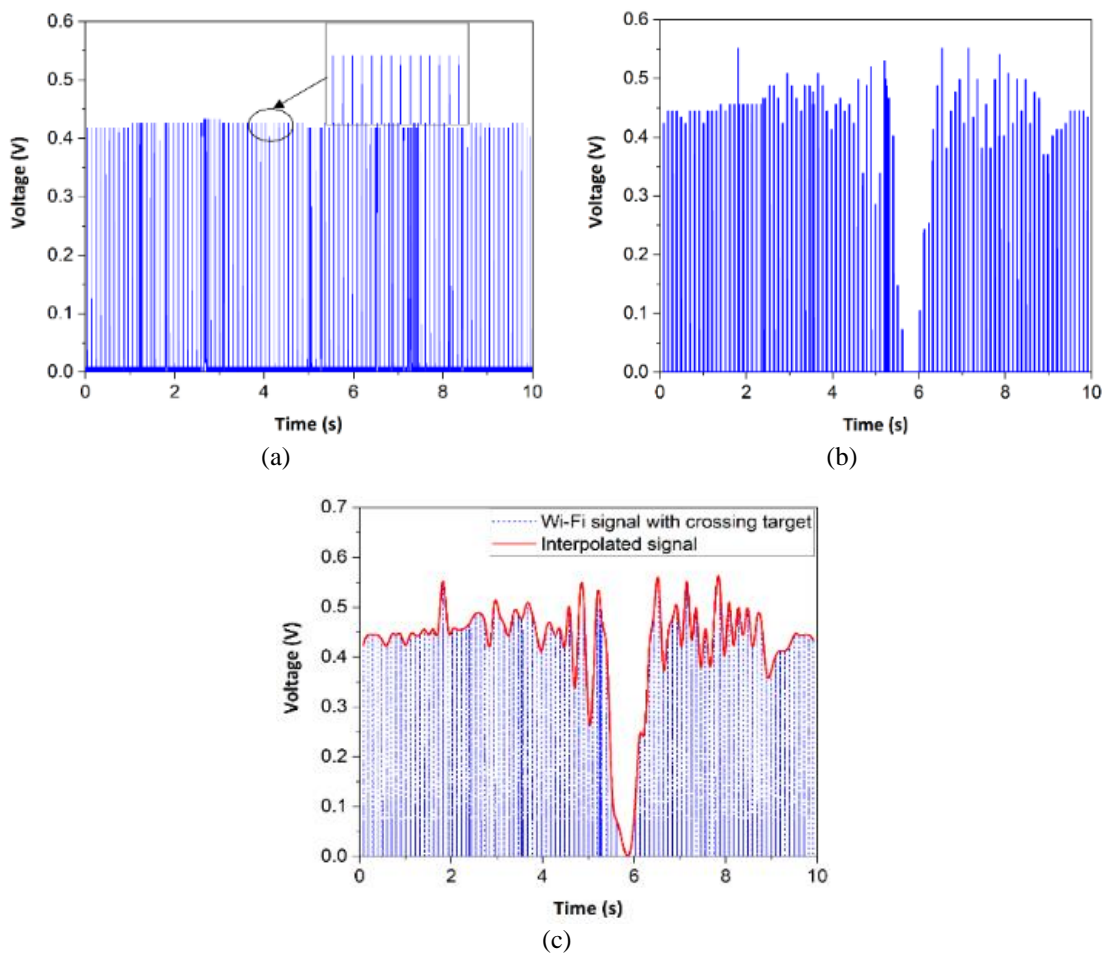


Figure 4. Raw pulsed Wi-Fi signal (a) without the presence of a target. Inset: pulsed signals, (b) with a target crossing the baseline, and (c) interpolated signal (red line)

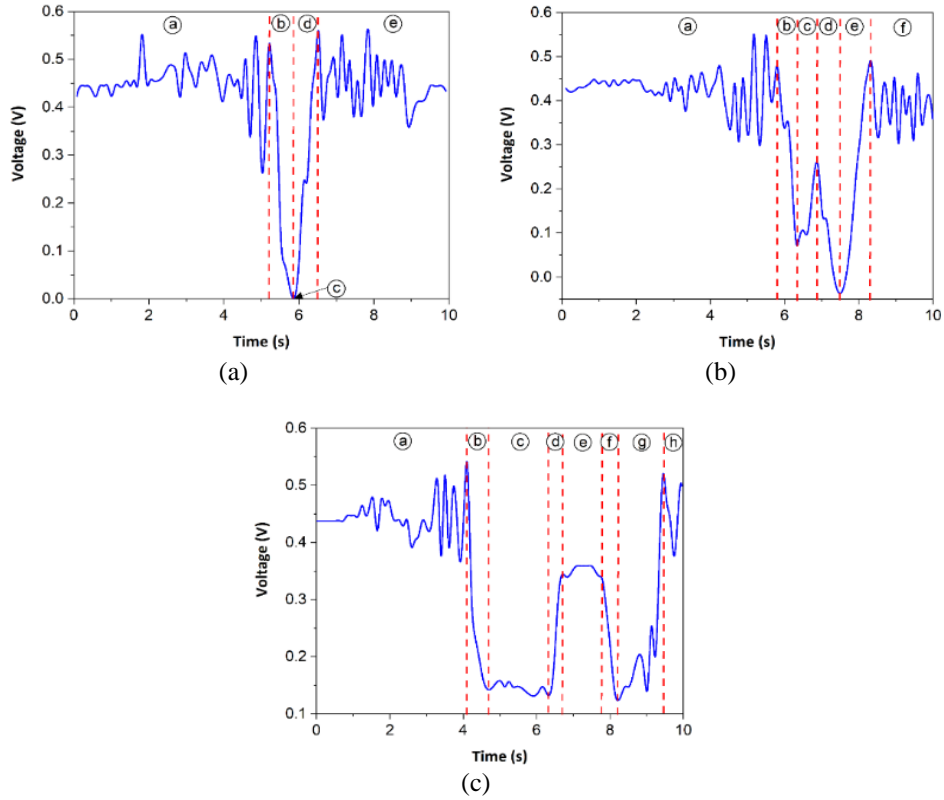


Figure 5. Time domain Doppler signal (a) walking, (b) bending, and (c) sitting

Table 1. Signature of human movements

Figure 5	Activity	Time domain description							
		(a)	(b)	(c)	(d)	(e)	(f)	(g)	(h)
(a)	Walking	Walking	Approaching baseline	Crossing baseline	Leaving baseline	Walking			
(b)	Bending	Walking	Approaching baseline	Bending down	Standing up	Leaving baseline	Walking		
(c)	Sitting	Walking	Approaching baseline	Moving to chair	Sitting down	Leaning on chair	Standing up	Leaving baseline	Walking

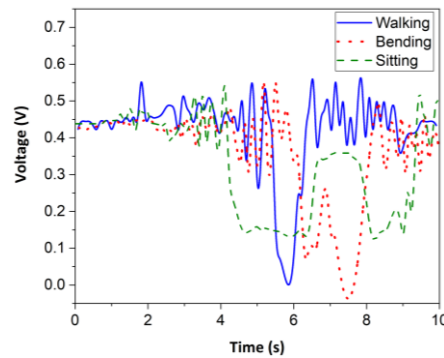


Figure 6. Comparison of Doppler signals

To examine the consistency of the signature, a total of 96 samples of each activity collected in the time domain as shown in Figure 6 are transformed into a frequency domain, where the sample's characteristics, presented in the main and side lobe forms, can be observed clearly. Figures 7(a) to (c) show the first 30 Hz of the frequency domain of 96 samples, where the main and side lobes can be observed, for

walking, bending, and sitting activities. From the figure, no obvious changes, and fluctuations in the voltage intensity as well as the shape of the main lobe are observed for 96 samples of each activity. This indicates that the participants engaged in the same activity and the signature is convincing and consistent even if it is performed by a different individual. Meanwhile, there is a fluctuation of waves in the side lobes generated by variable speeds of activity performance as well as other motions from minor parts of the body.

Figure 8 illustrates the first 10 Hz of the frequency domain for all 3 activities, which portrays a significant signature distinction between the activities. In order to do the classification, the features of the signature are extracted manually where 4 divisions are selected with the same range of frequency, as plotted in red dotted lines. As the signals in the frequency domain appear to begin at 1 Hz and the noise signals appear to begin at 9 Hz, therefore, the features are divided equally into 4 divisions with a range of 2 Hz. The first division is from 1 to 3 Hz, while the second division is from 3 to 5 Hz. The third division is divided from 5 to 7 Hz and the last division is from 7 to 9 Hz. In each division, the distinction range of the voltage intensity and frequency components for each activity are identified to classify the activities.

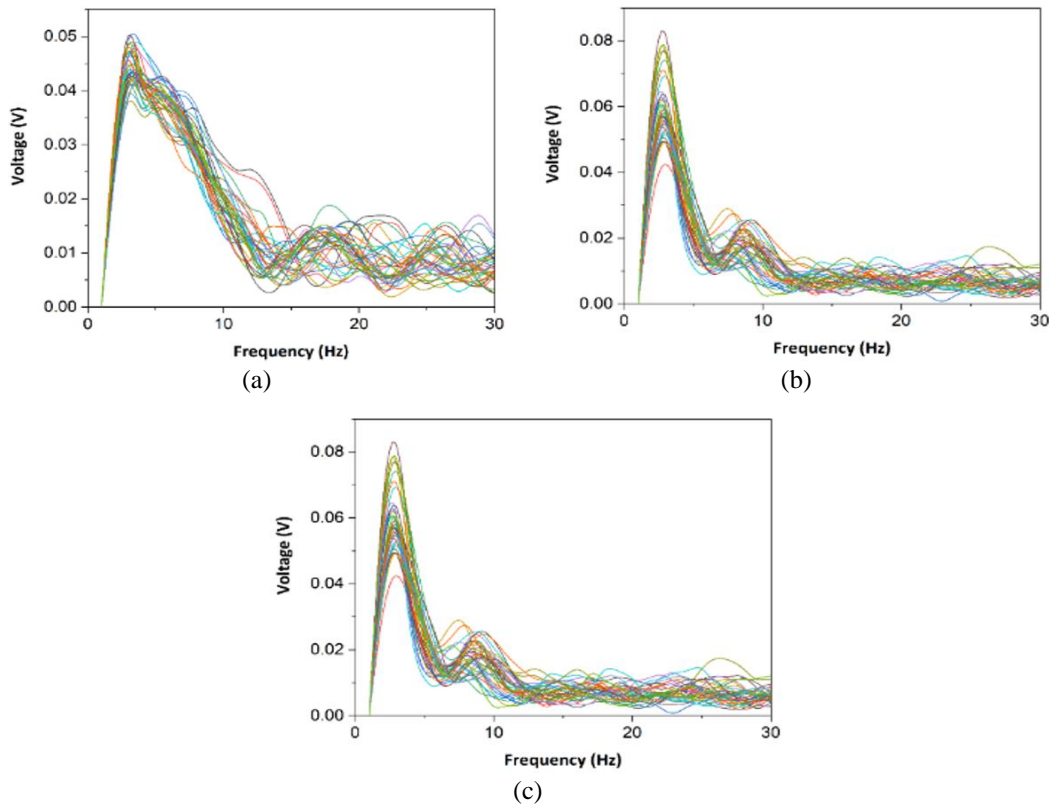


Figure 7. Frequency domain signals for 96 samples (a) walking, (b) bending, and (c) sitting

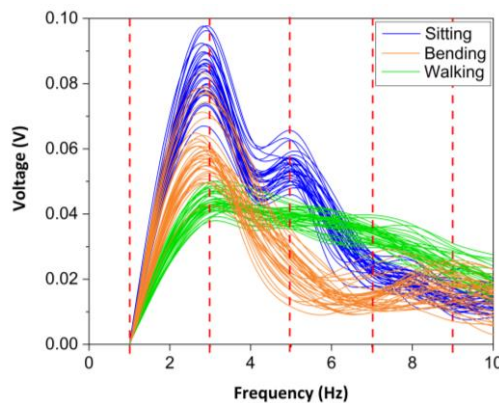


Figure 8. Comparison of frequency domain signals for 3 activities and 4 divisions of feature extractions

Figure 9 shows the centroid-based features from the 4 divisions with Figure 9(a) first, Figure 9(b) second, Figure 9(c) third, and Figure 9(d) fourth division. The walking features are presented in blue color, the sitting features are presented in red color, and the bending features are presented in green color. From the figure, it can be seen that there is a good separation between walking classes with sitting and bending classes. However, there are certain points when the walking class breaks away from the group and overlaps with those 2 classes. This is due to overlapping signals of walking activity in the frequency domain with signals of bending and walking activities. On the other hand, sitting and bending classes appear to be highly overlapping. This is because the signals from both activities in the frequency domain are closer to one other and have intersections.

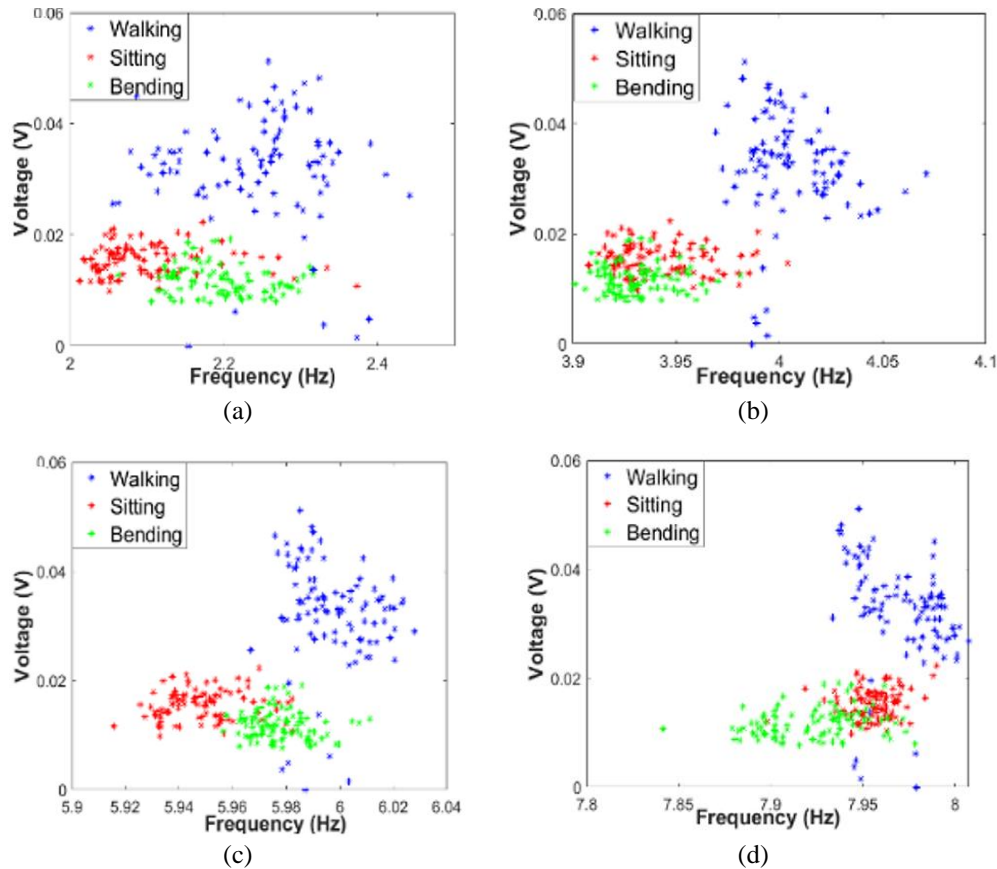


Figure 9. Comparison of frequency domain signals for three (3) activities and four (4) divisions of feature extractions: (a) first, (b) second, (c) third, and (d) fourth division

The confusion matrix's diagonal elements (green boxes) represent successfully categorized events, whereas the non-diagonal elements (pink boxes) represent inaccurate or misclassified events. The column and row of the confusion matrix represent the target and output class, respectively. As can be observed in Figure 10(a), for the walking target class in the first column, out of 96 tests, 1 element is misclassified into the bending class, yielding a classification accuracy of 99.0%. The second column, which represents the sitting target class, shows that there are 1 and 2 elements misclassified into the walking and bending classes, respectively, which results in 96.9% of classes being correctly classified. This is due to the inclusion of walking exercises as well as the resemblance of lowering the body from bending action. On the other hand, 3 elements are misclassified into the sitting class for the bending target class, resulting in a classification accuracy of 96.9%. This is due to a result of the bending activity including lowering the body action that is similar to sitting activity. The last column of the confusion matrix displays the algorithm's classification precision with 99.0%, 95.9%, and 97.9% for the activities of walking, sitting, and bending, respectively. The classifier has an overall accuracy of 97.6%, which is considered a relatively good result compared to the study carried out by [28] with a success rate of 78%, and in study [29] with a recognition accuracy of 84.65% with the ANN classification algorithm.

The classification accuracy using the KNN algorithm as shown in Figure 10(b) shows that there are 3 and 1 element are misclassified into the sitting and bending classes, respectively, for the walking target class, yielding a classification accuracy of 95.8%. 2 and 3 elements are misclassified into the walking and bending classes, respectively, for the sitting target class, resulting in 94.8% of classes being correctly classified. For the bending target class, however, 3 and 2 elements are misclassified into the walking and sitting classes, respectively, yielding a classification accuracy of 94.8%. The algorithm's classification precision for walking, sitting, and bending are 94.8%, 94.8%, and 95.8%, respectively. The classifier has an overall accuracy of 95.1%, which is comparable with the study carried out by [30] with 95.8% recognition accuracy and [31] with a classification rate of 96% using KNN classifier. Based on the two classifiers, the system may function well because the classification accuracy of both classifiers is greater than 95%.

Output class	Walking	95 33.0%	1 0.3%	0 0.0%	99.0% 1.0%
	Sitting	1 0.3%	93 32.3%	3 1.0%	95.9% 4.1%
	Bending	0 0.0%	2 0.7%	93 32.3%	97.9% 2.1%
		99.0% 1.0%	96.9% 3.1%	96.9% 3.1%	97.6% 2.4%
	Walking	Sitting	Bending		
	Target class				

(a)

Output class	Walking	92 31.9%	2 0.7%	3 1.0%	94.8% 5.2%
	Sitting	3 1.0%	91 31.6%	2 0.7%	94.8% 5.2%
	Bending	1 0.3%	3 1.0%	91 31.6%	95.8% 4.2%
		95.8% 4.2%	94.8% 5.2%	94.8% 5.2%	95.1% 4.9%
	Walking	Sitting	Bending		
	Target class				

(b)

Figure 10. Confusion matrix illustrating the accuracy of all activities expressed as a number of elements and percentages with (a) ANN and (b) KNN classifiers

4. CONCLUSION

In this experiment, Wi-Fi pulse signals are used as an illuminator of opportunity to identify and categorize 3 daily human actions, namely walking, bending, and sitting, conducted by 4 distinct people with equal body proportions and heights. ANN classifier has been employed to classify the signals and trained using the LOOCV method. The results clearly reveal a different Doppler signal between all activities, with an overall classification accuracy of 97.6%. It may be inferred that the PWR is capable of detecting distinct human motions even when conducted by different persons with equivalent body sizes and heights. The obtained accuracy also shows that the PWR system used in this work is reliable even without the reference channel and additional algorithms.

ACKNOWLEDGEMENTS

The authors would like to thank Microwave Research Institute (MRI) and Research Management Center (RMC), Universiti Teknologi MARA for all the support.

REFERENCES




- [1] I. Milani, F. Colone, C. Bongioanni, and P. Lombardo, "WiFi emission-based vs passive radar localization of human targets," in *2018 IEEE Radar Conference*, 2018, pp. 1311–1316, doi: 10.1109/RADAR.2018.8378753.
- [2] P. E. Howland, "Target tracking using television-based bistatic radar," *IEE Proceedings: Radar, Sonar and Navigation*, vol. 146, no. 3, pp. 166–174, 1999, doi: 10.1049/ip-rsn:19990322.
- [3] H. D. Griffiths and N. R. W. Long, "Television-based Bistatic radar," *IEE Proceedings F: Communications Radar and Signal Processing*, vol. 133, no. 7, pp. 649–657, 1986, doi: 10.1049/ip-f-1.1986.0104.
- [4] D. K. P. Tan, H. Sun, Y. Lu, M. Lesturgie, and H. L. Chan, "Passive radar using global system for mobile communication signal: theory, implementation and measurements," *IEE Proceedings: Radar, Sonar and Navigation*, vol. 152, no. 3, pp. 116–123, 2005, doi: 10.1049/ip-rsn:20055038.
- [5] P. Samczynski, K. Kulpa, M. Malanowski, P. Krysiak, and Maślakowski, "A concept of GSM-based passive radar for vehicle traffic monitoring," *2011 Microwaves, Radar and Remote Sensing Symposium, MRRS*, pp. 271–274, 2011, doi: 10.1109/MRRS.2011.6053652.
- [6] J. E. Palmer, H. Andrew Harms, S. J. Searle, and L. M. Davis, "DVB-T passive radar signal processing," *IEEE Transactions on Signal Processing*, vol. 61, no. 8, pp. 2116–2126, 2013, doi: 10.1109/TSP.2012.2236324.
- [7] P. Falcone, F. Colone, and P. Lombardo, "Potentialities and challenges of WiFi-based passive radar," *IEEE Aerospace and Electronic Systems Magazine*, vol. 27, no. 11, pp. 15–26, 2012, doi: 10.1109/MAES.2012.6380822.
- [8] B. Tan, K. Woodbridge, and K. Chetty, "A real-time high resolution passive WiFi Doppler-radar and its applications," in *2014 International Radar Conference, Radar 2014*, 2014, pp. 1–6, doi: 10.1109/RADAR.2014.7060359.
- [9] B. Tan, K. Woodbridge, and K. Chetty, "A wireless passive radar system for real-time through-wall movement detection," *IEEE Transactions on Aerospace and Electronic Systems*, vol. 52, no. 5, pp. 2596–2603, 2016, doi: 10.1109/TAES.2016.140207.
- [10] F. Colone, K. Woodbridge, H. Guo, D. Mason, and C. J. Baker, "Ambiguity function analysis of wireless LAN transmissions for passive radar," *IEEE Transactions on Aerospace and Electronic Systems*, vol. 47, no. 1, pp. 240–264, 2011, doi: 10.1109/TAES.2011.5705673.
- [11] A. Harcourt, G. Christou, and S. Simpson, *802.11ax: technical standards-making, the unlicensed spectrum, and the future of WiFi*, Global Standard Setting in Internet Governance, pp. 102–121, 2020, doi: 10.1093/oso/9780198841524.003.0006.
- [12] P. Bahl and V. N. Padmanabhan, "RADAR: an in-building RF-based user location and tracking system," in *Proceedings - IEEE INFOCOM*, 2000, vol. 2, pp. 775–784, doi: 10.1109/infcom.2000.832252.
- [13] C. Tang, W. Li, S. Vishwakarma, K. Chetty, S. Julier, and K. Woodbridge, "Occupancy detection and people counting using WiFi passive radar," *2020 IEEE Radar Conference (RadarConf20)*, 2020, doi: 10.1109/RadarConf2043947.2020.9266493.
- [14] H. Sun, L. G. Chia, and S. G. Razul, "Through-wall human sensing with WiFi passive radar," *IEEE Transactions on Aerospace and Electronic Systems*, vol. 57, no. 4, pp. 2135–2148, 2021, doi: 10.1109/TAES.2021.3069767.
- [15] H. El Zein, F. Mourad-Chehade, and H. Amoud, "Intelligent real-time human activity recognition using Wi-Fi signals," in *2023 International Conference on Control, Automation and Diagnosis, ICCAD 2023*, 2023, pp. 1–5, doi: 10.1109/ICCAD57653.2023.10152429.
- [16] I. Elujide, J. Li, A. Shiran, S. Zhou, and Y. Liu, "A real-time object detection for WiFi CSI-based multiple human activity recognition," in *Proceedings - IEEE Consumer Communications and Networking Conference, CCNC*, 2023, pp. 549–554, doi: 10.1109/CCNC51644.2023.10059647.
- [17] A. K. Sahoo, V. Kompally, and S. K. Udgata, "Wi-Fi sensing based real-time activity detection in smart home environment," *APSCON 2023-IEEE Applied Sensing Conference, Symposium Proceedings*, pp. 1–3, 2023, doi: 10.1109/APSCON56343.2023.10101249.
- [18] W. Li, B. Tan, and R. Piechocki, "Passive radar for opportunistic monitoring in E-health applications," *IEEE Journal of Translational Engineering in Health and Medicine*, vol. 6, pp. 1–10, 2018, doi: 10.1109/JTEHM.2018.2791609.
- [19] W. Li, B. Tan, and R. J. Piechocki, "WiFi-based passive sensing system for human presence and activity event classification," *IET Wireless Sensor Systems*, vol. 8, no. 6, pp. 276–283, 2018, doi: 10.1049/iet-wss.2018.5113.
- [20] X. Wang *et al.*, "Placement matters: understanding the effects of device placement for WiFi sensing," in *Proceedings of the ACM on Interactive, Mobile, Wearable and Ubiquitous Technologies*, 2022, vol. 6, no. 1, pp. 1–25, doi: 10.1145/3517237.
- [21] J. Sadowski, "When data is capital: datafication, accumulation, and extraction," *Big Data and Society*, vol. 6, no. 1, pp. 1–12, 2019, doi: 10.1177/2053951718820549.
- [22] J. R. Saura, B. R. Herraiz, and A. Reyes-Menendez, "Comparing a traditional approach for financial brand communication analysis with a big data analytics technique," *IEEE Access*, vol. 7, pp. 37100–37108, 2019, doi: 10.1109/ACCESS.2019.2905301.
- [23] Y. Du, J. Yue, Y. Ji, and L. Sun, "Exploration of optimal Wi-Fi probes layout and estimation model of real-time pedestrian volume detection," *International Journal of Distributed Sensor Networks*, vol. 13, no. 11, 2017, doi: 10.1177/1550147717741857.
- [24] P. Heckbert, "Fourier transforms and the fast fourier transform (FFT) algorithm," *Notes Computer Graphics*, vol. 3, no. 2, pp. 15–463, 1995.
- [25] S. J. Kwon, "Artificial neural networks," in *Artificial Neural Networks*, 2011, pp. 1–426.
- [26] P. Cimiano and H. S. Pinto, "Lecture notes in computer science (including subseries lecture notes in artificial intelligence and lecture notes in bioinformatics): preface," in *Lecture Notes in Computer Science (including subseries Lecture Notes in Artificial Intelligence and Lecture Notes in Bioinformatics)*, 2010, vol. 6317, pp. 431–440, doi: 10.1007/978-3-642-16438-5.
- [27] S. Bhat, A. Mukhopadhyay, and B. K. Sandhya Rani, "Dynamic media selection between WiFi and LTE in telemedicine scenarios," in *2017 International Conference on Advances in Computing, Communications and Informatics*, 2017, pp. 601–606, doi: 10.1109/ICACCI.2017.8125906.
- [28] K. K. Jung, J. W. Kim, H. K. Lee, S. B. Chung, and K. H. Eom, "EMG pattern classification using spectral estimation and neural network," in *Proceedings of the SICE Annual Conference*, 2007, pp. 1108–1111, doi: 10.1109/SICE.2007.4421150.
- [29] S. Chernbumroong, A. S. Atkins, and H. Yu, "Activity classification using a single wrist-worn accelerometer," in *5th International Conference on Software, Knowledge Information, Industrial Management and Applications*, 2011, pp. 21–25, doi:

10.1109/SKIMA.2011.6089975.




- [30] H. Zou, Y. Zhou, J. Yang, H. Jiang, L. Xie, and C. J. Spanos, "WiFi-enabled device-free gesture recognition for smart home automation," in *IEEE International Conference on Control and Automation*, 2018, pp. 476–481, doi: 10.1109/ICCA.2018.8444331.
- [31] M. G. Amin, Z. Zeng, and T. Shan, "Hand gesture recognition based on radar micro-doppler signature envelopes," in *2019 IEEE Radar Conference*, 2019, no. April, doi: 10.1109/RADAR.2019.8835661.

BIOGRAPHIES OF AUTHORS






Hidayatusherlina Razali    received a bachelor of engineering (Hons) in electronics from Universiti Teknologi MARA (UiTM) in 2019. She is currently pursuing her doctoral studies in the Faculty of Electrical Engineering, UiTM. Her research interests center on radar technology, with a particular emphasis on its application to the detection of human movement which focuses on both the hardware and signal processing components. She can be contacted at email: hida.sherlina@gmail.com.






Nur Emileen Abd Rashid    is currently a senior lecturer at University Technology MARA. She obtained her bachelor of electrical engineering from the Universiti Kebangsaan Malaysia in 2001 and subsequently her M.Sc. in computer, communication and human centered engineering from the University of Birmingham, UK in 2002. She pursued her studies and received her PhD in 2011 from the same university. She has contributed much of her expertise in areas related to radar technology, telecommunication signal processing and clutter modelling. Currently, she is attached to the Microwave Research Institute as a member and an active member of IET, IEEE and MyRAN. She can be contacted at email emileen98@uitm.edu.my.






Muhammad Nazrin Farhan Nasarudin    obtained a bachelor of engineering (Hons) in electronics in 2021 from University Teknologi MARA, Shah Alam and currently pursued PhD study in the same university. His PhD thesis involves several methods in radar technology for human movement detection including signal processing, feature extraction, and classifier algorithms. Currently he is working on advanced intelligence classifiers i.e. convolutional neural network and hybrid classifiers. He can be reached at email: nazrinfarhan98@gmail.com.






Nor Najwa Ismail    obtained a bachelor of engineering (Hons) in electronics (Communication) from the Faculty of Electrical Engineering, Universiti Teknologi MARA in 2012. In 2018, she obtained her Ph.D. from the Faculty of Electrical Engineering at UiTM Shah Alam via an accelerated program. Her research interests include wireless sensor networks, signal processing, and optic fiber laser. She can be reached at email najwaismail@uitm.edu.my.






Zuhani Ismail Khan    is an electrical and electronic engineer, graduated from University of Bradford, UK in 1998. After joining UiTM in the year 2000, she pursued her MSc in computer and information engineering at International Islamic University Malaysia and completed it in 2005. She then completed her PhD in electrical engineering at Universiti Teknologi MARA, UiTM in 2015 where she was involved in designing RF filters. Her research background concentrates on microwave and RF devices for high frequency systems. On October 2019 she was appointed as the member of Microwave Research Institute (MRI) and currently she holds the post of director of the institute. She can be contacted at email zuhani629@uitm.edu.my.






Siti Amalina Enche Ab Rahim    received the Diplôme d'Ingénieur in electronics and communications engineering from Ecole National Supérieur d'Electronique et de Radioelectricite de Grenoble (ENSERG), Grenoble, France in 2008 and received her D.Eng in electrical and electronics engineering from Kyushu University, Japan in 2017. In 2009, she joined Telekom Research and Development Sdn. Bhd (TMRND), Cyberjaya, Malaysia as a researcher, before joining Universiti Teknologi Mara, (UiTM), Shah Alam, Malaysia as a lecturer in 2017. Her current research interests include the design of RF passive components and RF CMOS integrated circuits. She can be reached at email: amalinaabr@uitm.edu.my.



Megat Syahirul Amin Megat Ali    is an Associate Professor at the College of Engineering, Universiti Teknologi MARA. He received his B.Eng. (Biomedical) from University of Malaya, Malaysia, in 2006. Then, in 2007, he obtained M.Sc. in Biomedical Engineering from University of Surrey, United Kingdom. He received his Ph.D. in Electrical Engineering from Universiti Teknologi MARA, Malaysia, in 2018. Dr. Megat is a Chartered Engineer, registered with the Engineering Council, United Kingdom, and Senior Member of the Institute of Electrical and Electronics Engineers. He is currently the Deputy Director at the Microwave Research Institute, Universiti Teknologi MARA, Malaysia. His main research interests are in applications of signal processing and machine learning for solving engineering problems. He can be contacted at email megatsyahirul@uitm.edu.my.



Nor Ayu Zalina Zakaria    is currently a Senior Lecturer at the School of Electrical Engineering, College of Engineering, Universiti Teknologi MARA, Malaysia, with nearly 16 years of engineering education experience. In 2017, she received her PhD in Radar Technology from the University of Birmingham in the United Kingdom. She received her BEng (Hons) in Electronics and Telecommunication Engineering from University Malaysia Sarawak and Master in Mobile and Satellite Communication Engineering from University of Surrey, United Kingdom in 2000 and 2003 respectively. Her areas of interest mainly in radar technology particularly, radar detection and related work in clutter analysis for forward scatter radar. She can be reached at email norayu713@uitm.edu.my.